Experimental study of friction noise of dry contact under light load

A. Le Bot – H. Ben Abdelounis – H. Zahouani

Laboratoire de tribologie et dynamique des systèmes
École centrale de Lyon, LTDS, 69134 Ecully Cedex, FRANCE
alain.le-bot@ec-lyon.fr

ABSTRACT. *This study is concerned with the measurement of friction noise radiated from the contact area of two sliding solids. The domain of interest is dry contact under light pressure where the roughness of surfaces is of a great importance. The modal properties of solids, explained by a numerical modal analysis, behave like a filter applied to the excitation signal. The friction mechanism is characterized by two effects. The contact stiffness coupling opposite pieces is determined by measuring the eigenfrequency shift. And the level of frictional forces is determined from measurement of power spectrum density of acceleration by deconvolution.*

RÉSUMÉ. *Cette étude concerne la mesure du bruit de frottement émis par la zone de contact de deux solides en mouvement. Le domaine exploré est celui du contact sec sous faible pression où la rugosité joue un rôle essentiel. Les propriétés modales des solides, connues par une analyse modale numérique, se comportent comme un filtre appliqué au signal d'excitation. Le mécanisme de friction est caractérisé par deux effets. La raideur de contact entre les pièces opposées est déterminée par le décalage des fréquences propres. Et le niveau des forces de friction est déterminé par déconvolution à partir des mesures de densité spectrale de puissance d'accélération.*

KEYWORDS: *friction noise - sound radiation - roughness*

MOTS-CLÉS : *bruit de frottement - rayonnement sonore - rugosité*

1. Introduction

Friction sound may occur in a wide variety of situations. Brakes squeal of cars or trains, all musical instruments such as violins, guitars, sound radiated by glass when rubbing a moist finger, tyres on road and so on. This wide variety of examples hide in fact a so large variety of physical phenomenons. For an overview of friction sound, see (Akay 2002).

In this study, we are interested in roughness sound, that is the friction sound arising when two dry and rough surfaces are rubbed on each other under light normal load. In such a situation, the sound is produced in three steps. Firstly, the interaction of rough surfaces during the relative movement generates many shocks of opposite asperities. Secondly, the whole structure loaded by interaction forces, vibrates on its own eigenmodes. Finally, the sound is radiated from structure and then reaches the receiver point. This study investigates steps 2 and 3 in experimental and numerical ways, but does not provide a theory for the generation mechanism (step 1). However, it aims to provide a method for measuring the interaction forces and contact stiffness, an essential condition to understand step 1.

The experiment carried out in this study was first proposed in (Maruyama *et al.*, 2004). This is an attempt to understand the relationship between roughness and sound with the simplest pieces. Another related experiment on frictional sound may also be mentioned (Othman *et al.*, 1990-1) and an original device for measuring the roughness from sound is proposed in (Othman *et al.*, 1990-2).

2. Description of the experiment

Following the study of (Maruyama *et al.*, 2004), two sheets of steel are applied on each other. A sliding movement generates the friction and also the noise (Fig. 1). The movement is applied by hand with a loading force approximately controlled and with a sliding speed which has been measured. The sound produced by the friction is recorded with a microphone and a digital I/O board PCI-DAS-6013 16 bits in an anechoic chamber. The power spectrum density is obtained with $N = 1024$ lines with a Hanning time window. All details of the experimental implementation can be found in (Maruyama *et al.*, 2004).

The pieces are made of hot rolled steel of common usuage (S235JRG2). This is a ferritic steel whose mechanical characteristics are the followings. Young's modulus $E = 210$ GPa at $20°$C, Poisson's coefficient $\nu = 0.3$, tensile strength $R_m = 370$ Mpa and yield strength $R_e = 235$ Mpa. The pieces have a parallelepipedic shape with length 80 mm, width 19 mm and thicknesses 3.9 mm, 6.2 mm and 8 mm. The surfaces are prepared by milling for the most rough surface and by polishing for the others. In Table 1 are shown the roughnesses R_z and R_a of the four surfaces. R_a is as usual defined as the arithmetic mean value of the roughness profile and R_z is the average of five peak-valley heights.

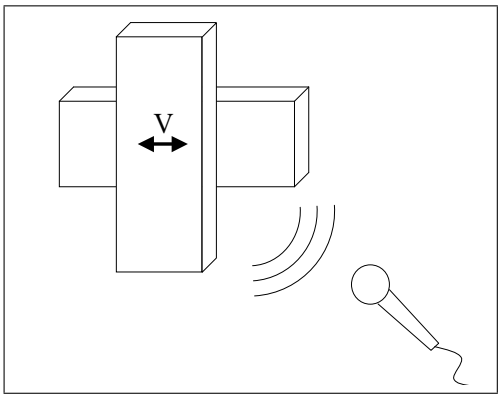

Figure 1. *Two pieces of metal are rubbed on each other in transverse direction and the friction sound is recorded with a microphone in an anechoic chamber.*

name	milled	80	400	1200
R_z	11.5 μm	1.2 μm	0.6 μm	0.5 μm
R_a	2.3 μm	0.2 μm	0.1 μm	0.08 μm

Table 1. *Roughness of sheets measured with profilometer.*

The measured friction noise has a very large band spectrum. In Figure 2 is shown the signal spectrum measured with a 1/4" microphone and a high sample frequency ($f_e = 200$ kHz). This microphone has a very high limiting frequency at 70 kHz well-suited for the determination of the noise upper frequency. The noise spectrum is found to extend up to 45 kHz. Beyond this limit, the friction noise level is comparable to the background noise level although the actual friction noise spectrum is certainly wider than it can be measured. As we are only interested in audible noise, all measurements of this study were confined into the audio band 20 Hz - 20 kHz by using an anti-aliasing filter and a sample frequency of $f_e = 60$ kHz. A 1/2" free-field microphone type B&K 4189 having a higher sensibility than the 1/4" microphone has been prefered. It is better suited for high quality measurements.

3. Modal behavior and contact stiffness

A numerical modal analysis was performed with a finite element software for a parallelepipedic sheet of steel with free boundary conditions. Four eigenfrequencies are found for $h = 6$ and 8 mm in the audio band and six eigenfrequencies for $h = 4$ mm. These eigenfrequencies are summarized in Table 2. The eigenvectors are shown in Figure 3. It is clear that the first eigenfrequency is always the first flexural mode (fz_1), the second eigenfrequency is the first torsional mode (tx_1), the third and

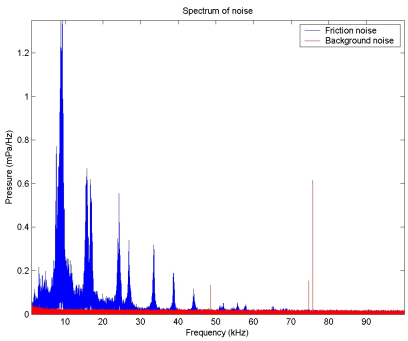

Figure 2. *Spectrum of the friction noise measured with a 1/4" microphone with limiting frequency 70 kHz, sample frequency 200 kHz,* $R_z = 11.5\ \mu m$ *and* $h = 4$ *mm.*

	fz_1	tx_1	fz_2	fy_1	tx_2	fz_3
$h = 3.9$ mm	3207	7644	8763	13506	15688	16935
$h = 6.2$ mm	5068	11219	13513	13533	> 20 kHz	> 20 kHz
$h = 8$ mm	6423	13415	16813	13520	> 20 kHz	> 20 kHz

Table 2. *Eigenfrequencies (Hz) by finite element method within the audio band.*

fourth eigenfrequencies are the first flexural mode in transverse direction (fy_1) and the second flexural mode (fz_2). The additional fifth and sixth eigenfrequencies for $h = 4$ mm are respectively the second torsional mode (tx_2) and the third flexural mode (fz_3).

The power spectrum density of friction noise has been measured for different loading forces, roughnesses and sliding speeds. Results are respectively shown in Figures 5, 6 and 7. The vertical thick lines point out the position of eigenfrequencies of uncoupled pieces computed by finite element method. We first remark that the eigenfrequencies computed by finite element method well match with the peaks of power spectrum density especially for low loading force, high roughness and high sliding speed. It means that the coupling between the two metal pieces is light and that the pieces behave like being totally uncoupled. This type of friction noise involving weak contacts of rough surfaces has been named roughness noise in (Akay 2002) Section II. But when the loading force increases (Figure 5), when the roughness decreases (Figure 6) or when the sliding speed decreases (Figure 7), the coupling become more important and the first eigenfrequency is shifted towards high frequencies.

In order to understand the shift of eigenfrequency, let consider that the interaction may be modelled as a single contact stiffness localized in the centre of the pieces as shown in Figure 4. The presence of this additional stiffness acts as a constraint and then results in an increase of eigenfrequency.

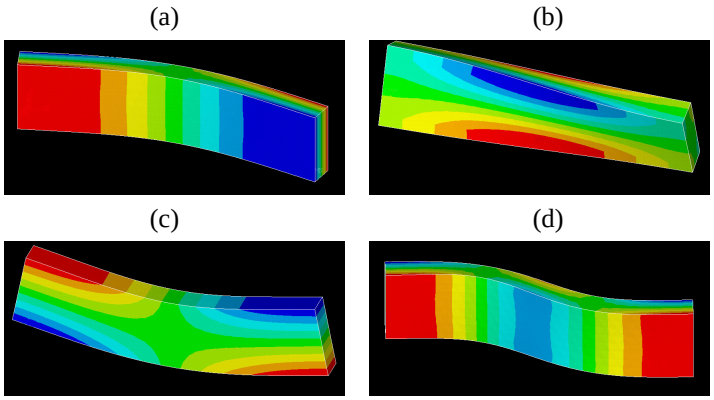

Figure 3. *Eigenmodes by finite element method. (a), First flexural mode fz_1. (b), First torsional mode tx_1. (c), First transverse flexural mode fy_1. (d), Second flexural mode fz_2.*

Mode 1 is more dependant on the coupling strenght than modes 2, 3 (which are almost one in Figs. 5-7) and 4. This phenomenon has been pointed out in (Maruyama *et al.*, 2004) and can be explained from the numerical modal analysis. Mode 1 is a flexural one and has a maximun of vibration at the centre of piece. This eigenfrequency is then highly dependant on the contact stiffness. Modes 2, 3 and 4 are the first torsional mode, the first transverse flexural mode and the second flexural mode. All of them have a node of vibration at the centre of the piece in normal direction. They are thus unaffected by the application of an additional rigidity (contact stiffness) at this point. This explains why these eigenfrequencies are not dependant on the contact conditions.

It is apparent from Figures 5, 6 and 7 that the contact stiffness increases with the static normal load, with the reciprocal of roughness and with the reciprocal of sliding speed. It possible to assess the contact stiffness. By applying the Rayleigh-Ritz method to the first eigenfrequency, the circular frequency ω' of the coupled system is such that equality of deformation energy and kinetic energy is verified,

$$D\int_0^l \psi''^2(x)\mathrm{d}x + k\psi^2(l/2) = m\omega'^2\int_0^l \psi^2(x)\mathrm{d}x, \qquad [1]$$

where $\psi(x) = \cosh\lambda x/l + \cos\lambda x/l - \sigma(\sinh\lambda x/l + \sin\lambda x/l)$ with $\sigma = 0.98$ and $\lambda = 4.73$, $l = 80$ mm being the length of the beam (Blevins 1979), is the first eigenmode for flexural wave of a single piece and k is the contact stiffness applying at $x = l/2$. $D = Eh^3/12(1-\nu^2)$ is the bending stiffness of the beam and m is the mass per unit length. The uncoupled eigenfrequency ω also verifies the equality of energies,

$$D\int_0^l \psi''^2(x)\mathrm{d}x = m\omega^2\int_0^l \psi^2(x)\mathrm{d}x. \qquad [2]$$

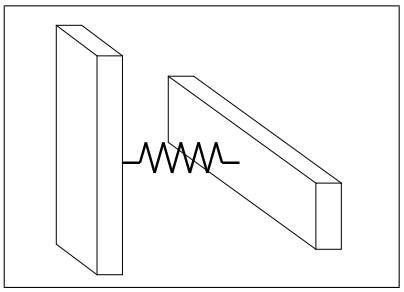

Figure 4. *Two sheets of metal separated by a contact stiffness acting in normal direction.*

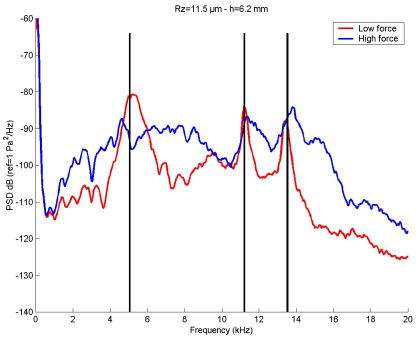

Figure 5. *Power spectrum density of friction noise for different loading forces.*

Thus, the contact stiffness is related to the frequency shift $\Delta\omega = \omega' - \omega$ with,

$$k = 2m\omega^2 \times \frac{\Delta\omega}{\omega} \times \frac{||\psi||^2}{\psi^2(l/2)}. \qquad [3]$$

with $||\psi||^2 = \int \psi^2 \mathrm{d}x$. An integration of the square of the above function ψ leads to $\psi^2(l/2)/||\psi||^2 = 1.97/l$. For instance, from Figure 6 the frequency shift of the first eigenmode is $\Delta\omega/\omega = 0.2$ between $R_z = 11.5$ and $R_z = 1.2$. leading to a contact stiffness $k = 15\ 10^6$ N/m.

4. Power spectrum density of exciting forces

As it has been pointed out, the sound power spectrum density is highly dependant on the modal behavior of the pieces being excited by friction. The question arising now is whether it is possible or not to investigate the effect of roughness independantly of the shape or mechanical properties of pieces. This is achieved by measuring (in an indirect way) the dynamical force level responsible of vibration and sound.

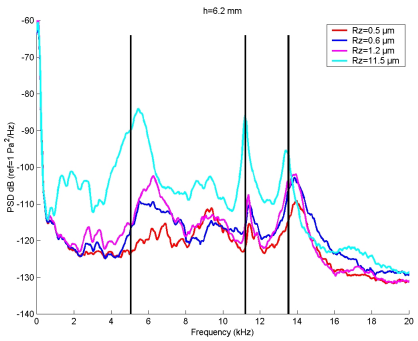

Figure 6. *Power spectrum density of friction noise for different roughnesses.*

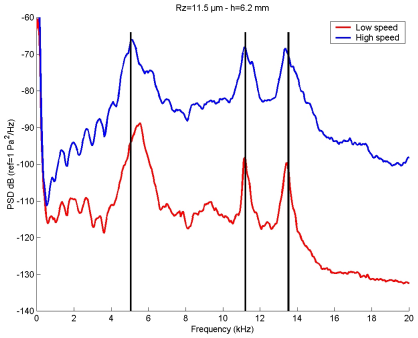

Figure 7. *Power spectrum density of friction noise for different sliding speeds.*

Assuming that the driving force $f(t)$ stemming from friction is a random function of time, the acceleration $a(t)$ at any receiver point on the structure is also a random function filtered by the modal behavior of the piece. If the filter is considered to be linear, the power spectrum density S_{aa} of the acceleration is related to the power spectrum density S_{ff} of the driving point by (Peebles 1987),

$$S_{aa}(\omega) = |H_{fa}(\omega)|^2 S_{ff}(\omega), \qquad [4]$$

where ω is the frequency and H_{fa} is the transfer function between the driving force at point x_0 and the acceleration at the receiver point x_1. This function may be known either by direct measurement or by numerical modal analysis with

$$H_{fa}(\omega) = \sum_{i=1}^{4} \frac{\omega^2}{M} \frac{\psi_i(x_0)\psi_i(x_1)}{\omega_i^2 + 2i\zeta_i\omega\omega_i - \omega^2}, \qquad [5]$$

where M is the mass of piece. The eigenmodes ψ_i and eigenfrequencies ω_i have been previously determined by finite element method. It is however difficult to predict the

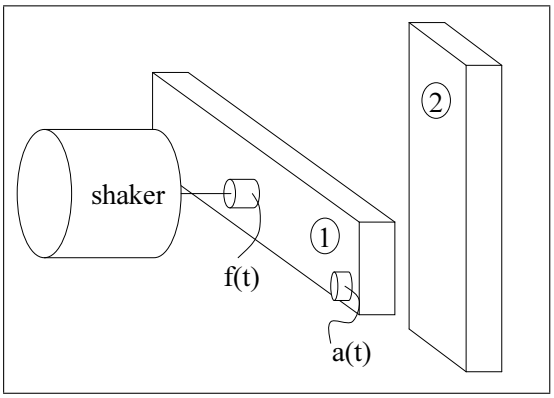

Figure 8. *The frequency response function of piece 1 is first measured between an accelerometer and a force probe under the shaker by applying a white noise. Secondly, the power spectrum density of acceleration is measured in same conditions by rubbing piece 2 on piece 1.*

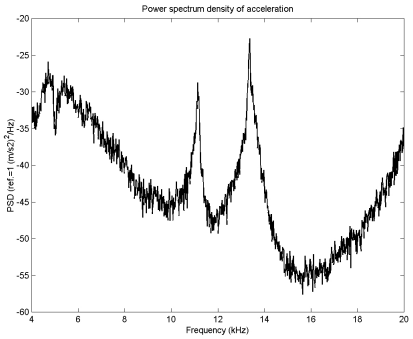

Figure 9. *Power spectrum density of acceleration.*

modal damping factors ζ_i without measurement. This is the reason why the experimental solution has been prefered. An accelerometer type B&K 4975 is positioned in a corner of the piece. This receiver point can catch three of the four modes. The frequency response function H_{fa} has been first measured with an electromagnetic shaker and a force probe type B&K 8001 with a white noise excitation within the audio band. Secondly, the acceleration power spectrum density has been measured by rubbing the other piece on the first one but without removing the shaker. This is important because when the frequency response function was measured, all modes of the isolated piece but also of the entire system including probes and shaker was captured. Then for an accurate deconvolution, the acceleration power spectrum density must be acquired in exactly same conditions.

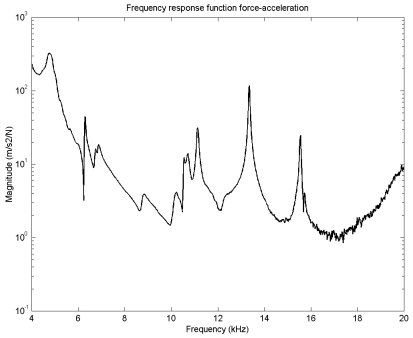

Figure 10. *Frequency response function force-acceleration.*

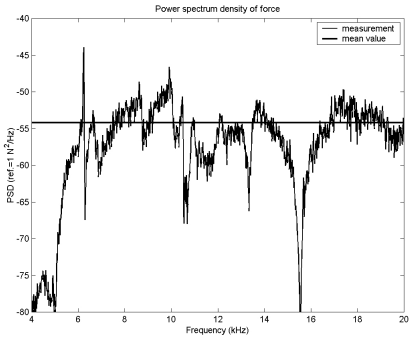

Figure 11. *Power spectrum density of dynamical contact force obtained by deconvolution.*

In Figures 9-11 is shown an example of force power spectrum density determined by this method. As expected, the power spectrum density of acceleration has some peaks corresponding to the eigenfrequencies of pieces but also to some additional eigenfrequencies of the entire system. These eigenfrequencies are more visible on the frequency response function. But, the power spectrum density obtained from Eq. (4) is more flat in the frequency band 5 kHz - 20 kHz although some holes are yet visible. A perfectly constant power spectrum density is typical for white noise. In case of Figure 11, a constant level of $S_{ff} = 4$ mN^2/Hz is obtained showing that the excitation by friction is an δ-correlated white noise and may be modelled by a "rain-on-the-roof" excitation.

Using this method, it has been found that the power spectrum density of force highly depend on the sliding speed and the roughness (increasing function) but less on the loading force. This result may be checked on the sound pressure level shown in Figs. 5, 6 and 7.

5. Conclusion

In this study, it has been shown how the noise emanating from rubbed rough surfaces depend on the modal properties of pieces in contact. Modes and eigenfrequencies of uncoupled pieces have been determined and well match with measurements showing that the coupling between opposite pieces remains light during contact. Then, it has been proposed to characterize the friction mechanism generating noise with two quantities.

First, the contact stiffness is responsible of a shift to high frequencies of the first flexural mode. The contact stiffness is related to this frequency shift by Eq. (3). It is found that the contact stiffness increases with the static normal load, with the reciprocal of roughness and with the reciprocal of sliding speed.

Secondly, the driving force level has been determined by a deconvolution from the measurement of the power spectrum density of acceleration and the frequency response function of the system. These forces are found to be closed to a "rain-on-the-roof" excitation. The roughness sound is thus a white noise filtered by the modal behavior of the piece. It increases with roughness and sliding speed but less with loading force.

Acknowledgements

The authors gratefully acknowledge Professor Kato for his visit and deep discussion on sound friction and Doctor Stoimenov to have engaged in correspondence on the same subject.

6. References

Akay A., "Acoustics of friction", *J. Acoust. Soc. Am.*, vol. 111, no. 2, 2002, p. 1525-1548.

Othman M.O., Elkholy A.H., Seireg A.A., "Experimental investigation of frictional noise and surface-roughness characteristics", *Experimental mechanics*, vol. 47, dec. 1990, p. 328-331.

Othman M.O., Elkholy A.H., "Surface-roughness measuring using dry friction noise", *Experimental mechanics*, vol. 47, sept. 1990, p. 309-312.

Maruyama S., Stoimenov B., Adashi K., Kato K., "The roughness effect on the frequency of frictional sound", *Proceedings of the 11th Nordic Symposium on Tribology NORDTRIB 2004*, Tromso, Norway, 1-4 June 2004, 9 pages.

Blevins R., *Formulas for natural frequency and mode shape*, Van Nostrand Reinhold Company, 1979.

Peebles JR., *Probability, random variables, and random signal principles*, Mc Graw Hill, 1987.